High-Performance Styrene Epoxidation with Vacancy-Defect Cobalt Single-Atom Catalysts

Boqian Jia, Lei Bai, Zheng Han, Ren Li, Junxiu Huangfu, Chongao Li, Jiming Zheng, Yunteng Qu, Kunyue Leng, Yi Wang, et al.

High-performance styrene epoxidation with vacancy-defect cobalt single-atom catalysts

Boqian Jia [‡, †], *Lei Bai* [†], *Zheng Han* [†], *Ren Li* [†], *Junxiu Huangfu* [†], *Chongao Li* [†], *Jiming Zheng* [†], *Yunteng Qu* [†], *Kunyue Leng* [*, †], *Yi Wang* [*, ‡, †], *and Jinbo Bai* [*, §]

[†] State Key Laboratory of Photoelectric Technology and Functional Materials, International Collaborative Center on Photoelectric Technology and Nano Functional Materials, Institute of Photonics and Photon-Technology, Northwest University, Xi'an, Shaanxi 710069, China

[§] Laboratory MSSMat, CNRS UMR 8579, Ecole CentraleSupélec, Université Paris-Saclay, 8-10 rue Joliot-Curie, Gif-sur-Yvette 91190, France

KEYWORDS: single-atom catalysts, cobalt, styrene epoxidations, tert-butyl hydroperoxide, styrene oxide

ABSTRACT: Exploring highly active and cost-effective catalysts for styrene epoxidation is of great significance, but it remains challenge to simultaneously achieve excellent conversion and selectivity towards styrene oxide. In this work, the structures and performance of Co, Fe and Cu single atom catalysts (SACs) in styrene epoxidation with TBHP are predicted by DFT calculations. The results reveal that the Co-N structure prefers to gain styrene oxide compared to Fe-N and Cu-N structures. This predicted result is verified via catalytic evaluations, where the Co SACs displayed significantly higher styrene oxide selectivity than Fe and Cu SACs. Moreover, the activity of Co SAC can be further improved by the construction of unsaturated vacancy-defect cobalt single sites. As a result, an excellent performance with a styrene conversion of 99.9% and a styrene oxide selectivity of 71% is achieved after a reaction time of 8 hours on the optimal Co SAC.

1. Introduction

As an important chemical, styrene oxide (SO) is widely used in the synthesis of plasticizer, epoxy resins and perfumes, and is also a key intermediate for the manufacture of pharmaceuticals and fine chemicals [1-4]. Commonly, SO is obtained via the chlorohydrin or Prilezhaev process, which is associate to hazardous wastes and environmental damage. [4-6] To this end, adopting green oxidants (e.g. O_2, H_2O_2 and tert-butyl hydroperoxide) to effectively steer epoxidation of styrene represents a promising strategy. [7-9] However, due to the direct oxidation of styrene (which produces benzaldehyde, as shown in Scheme 1), it is generally difficult to realize high SO selectivity on traditional catalysts. [8-16] Recently, single and dual atom catalysts have attracted greatly attentions in various applications, owing to their high atom utilization, remarkable novel catalytic activity, and conformational flexibility. [] In the epoxidation reactions, these catalysts are proven that can inhibit the direct oxidation path effectively. [1,2,4,17] Generally, noble metal-based catalysts simultaneously exhibit high conversion and selectivity for the epoxidation of styrene, [1,4] but their natural scarcity greatly inhibits their industrial application. In addition, even though non-noble metal-based catalysts exhibit epoxidation of styrene activity to some degree, a huge decline of SO selectivity will be observed due to the overoxidation of SO. [2] Therefore, it remains a significant challenge to acquire SO in an efficient and cost-effective manner.

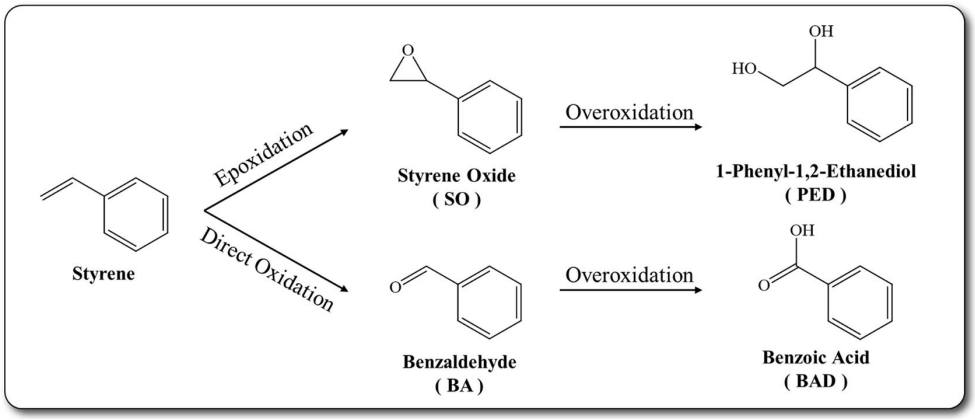

Scheme 1. Path diagram of styrene oxidation

Further, current investigations about atomic scale catalysts are primarily based on O_2 oxidant. As known, oxygen is a strong oxidizing agent, and the atomic scale catalysts can exhibit good activity in the reactions that involves O_2 dissociation, such as oxygen reduction reaction.[] However, probably due to the solubility of O_2 in the reaction system and the high O=O bond energy (498 kJ mol^{-1}) [Nature Communications, 2013, 4, 2076], a higher reaction temperature (such as 140 ℃ []) or longer reaction time (such as 12 hours []) is required in the studies combined with atomic scale catalysts and O_2 oxidants, which is unfavorable to industrial application and may lead to the severe overoxidation. From this perspective, it is necessary to employ other green oxidants, to reduce the undesirable operational conditions. Herein, we studied the performance of Fe, Co and Cu single atom catalysts (SAC) in styrene epoxidation with tert-butyl hydroperoxide (TBHP). Through the analysis of energy barriers to form SO and benzaldehyde (BA) using DFT calculations, we discovered that Co SAC with unsaturated Co-N_3 coordination may be more desirable for styrene epoxidation with TBHP. This predicted result was well verified by catalytic

evaluations. In the presence of the as-prepared Co SAC, an excellent styrene conversion (99.9%) and a high SO selectivity (71%) is achieved simultaneously.

2. Results and Discussion

According to the kinetics reported in the literatures, [11,15,18-21] a mechanism for selective oxidation of styrene is illustrated schematically in Figure 1 and Figure S1. First, TBHP molecule is adsorbed on the transition metal sites (TS1), resulting in the formation of metal oxo species (TS2), which is subsequently transformed into metal peroxo species (TS3) by another TBHP molecule.[11,15,21] The interaction between metal peroxo species and C=C bonds forms peroxo metallocycles (TS4).[11,18,20,21] Finally, the dissociation of peroxo metallocycles forms SO or benzaldehyde (BA).[15,19] Three commonly used SACs for oxidation reactions (i.e. Fe, Cu and Co SACs) are studied by density functional theory (DFT) calculations along this reaction route. As shown, Fe, Co and Cu SACs all exhibit a thermodynamically downslope from TS1 to TS4. For Fe SAC (Figure 1B), the formation of SO requires to overcome an energy barrier of 1.54 eV, which is higher than that of the BA (1.38 eV), suggesting the priority of BA formation. A similar result is observed over Cu SAC (Figure 1C). However, this tendency is reversed when the metal site is replaced by Co. As shown in Figure 1D, the energy barriers to form SO is 0.82 eV on Co SAC, which is less than that of BA (1.10 eV). In addition, the influence of the coordination number on Co SACs is studied. As shown in Figure 1E, the Co-N_3 structure maintains the priority of SO formation and observably reduces its energy barrier. Therefore, Co SACs with unsaturated Co-N_3 structure may be a more desirable catalyst for styrene epoxidation with TBHP.

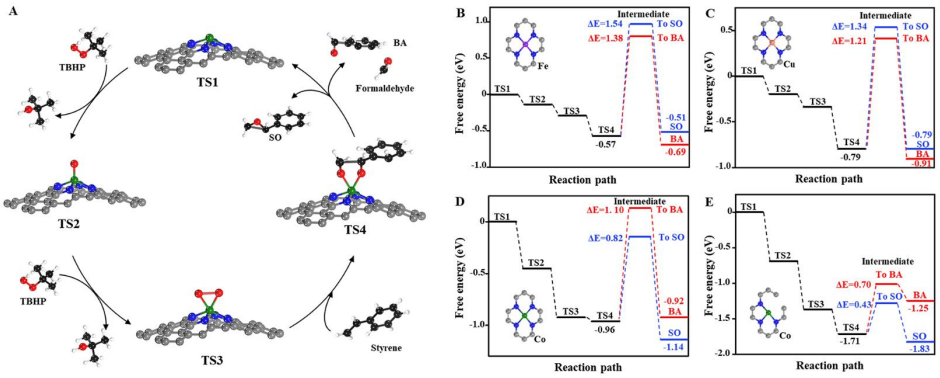

Figure 1. Theoretical study. (A) mechanism for the styrene epoxidation. Free energy diagrams for styrene epoxidation on (B) Fe-N_4, (C) Cu-N_4, (D) Co-N_4 and (E) Co-N_3 along the reaction pathway.

Based on the calculation results, Co SACs with different Co-N coordination environments are prepared through the traditional host-guest method, by alternating the pyrolysis temperature, [22,23] which are labelled as Cu/ZIF-800, Co/ZIF-900 and Co/ZIF-1000. The physical-chemical characteristics of these samples are shown in Table 1. Cu/ZIF-800, Co/ZIF-900 and Co/ZIF-1000 exhibit a Co loading of 2.38%, 2.53 % and 3.13 %, respectively. And, higher specific surface area is achieved at higher pyrolysis temperature, which is in line with previous reports. Figure 2 and Figure S2 show the TEM images of the various samples. All of them exhibit a dodecahedral rhombus shape with a particle size of approximately 200 nm. No metal nanoparticle can be observed in their corresponding HAADF-TEM images, energy dispersive spectroscopies (Figure 2 A-C) and selected area electron diffraction (Figure S2), suggesting homogeneous dispersion of Co in these samples. Aberration-corrected HAADF-STEM images of Co/ZIF-800 (Figure 2D and Figure S3), Co/ZIF-900

(Figure 2E and Figure S4) and Co/ZIF-1000 (Figure 2F and Figure S5) further confirm that Co atoms are homogeneous dispersed. The size of the bright spots is approximately 0.17 nm, which is consistent with the reported size of Co atomical sites.[24]

Table 1. textual properties and chemical composition.

Sample	Co (wt. %) [a]	S_{BET} (m^2g^{-1})	S_{micro} (m^2g^{-1}) [b]	S_{extern} (m^2g^{-1}) [b]	V_{micro} (cm^3g^{-1})	V_{meso} (cm^3g^{-1}) [c]
Co/ZIF-800	2.38	477.42	378.48	98.94	0.20	0.08
Co/ZIF-900	2.53	633.41	492.64	140.77	0.26	0.10
Co/ZIF-1000	3.13	815.00	570.79	244.22	0.30	0.17

[a] ICP-OES; [b] t-plot method; [c] BJH method (adsorption branch).

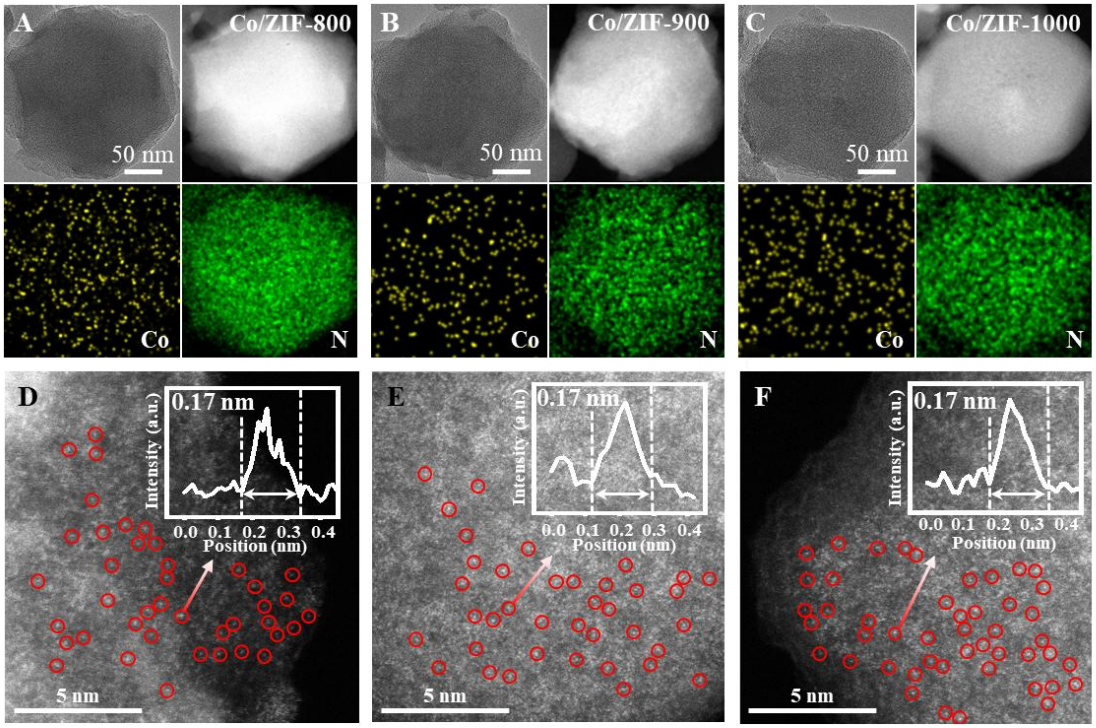

Figure 2. Characterizations of Co SACs. (A-C) TEM and HAADF-TEM images coupled with EDS mappings for Co/ZIF-800 (A), Co/ZIF-900 (B) and Co/ZIF-1000 (C). (D-F) HAADF-STEM images and the corresponding intensity profiles of Co/ZIF-800 (D), Co/ZIF-900 (E) and Co/ZIF-1000 (F).

Figure 3A shows the XRD patterns of Co/ZIF-800, Co/ZIF-900 and Co/ZIF-1000, where no characteristic peak of Co nanoparticles is detected, in line with the electron microscope results. The Co 2p XPS spectra of the various samples are shown in Figure S7. A broad peak centred at 780.2 eV is observed in all these three samples, which is situated between Co^0 (779.8 eV) and Co^{2+} (780.7eV). [25] Moreover, X-ray absorption fine structure (XAFS) spectroscopy is used to clarify the detailed structure of Co species in Co/ZIF-800, Co/ZIF-900 and Co/ZIF-1000. As shown in Figure 3B, they exhibit a stronger white-line intensity peak compared with Co foil, but their white-line intensities are lower than that of Co_2O_3 and cobalt (II) phthalocyanine, which is similar to the reported results [Nat. Catal. 2020, 3, 1044], again suggesting the partial positive charge of Co in these samples. Figure 3C shows the EXAFS spectra of Co/ZIF-800, Co/ZIF-900 and Co/ZIF-1000. The Co-N coordination at about 1.5 Å is detected in these samples, and the Co-Co coordination at approximately 2.2 Å and Co-O bond at about 1.6 Å are not detected, which is similar as that of cobalt (II) phthalocyanine, suggesting the formation of Co single sites. In comparison, the interatomic distance of Co-N and the intensity of the main peak in Co/ZIF-1000 are reduced compared with that of Co/ZIF-800 and Co/ZIF-900,

suggesting the lower coordination number for Co/ZIF-1000. Figure 3D and Table S1 show the fitting curves of their EXAFS spectra and the structural parameters extracted from the fitting curves, respectively, which indicates that Co/ZIF-1000 is the desirable Co SAC with unsaturated Co-N_3 coordination, Co/ZIF-800 is a Co SAC with Co-N_4 coordination structure, and Co/ZIF-900 is a mixture of Co-N_3 and Co-N_4 structures. More information about Co based SACs, such as the N_2 isotherms (Figure S8) and Raman spectra (Figure S9) are shown in the Supplementary Information. For further comparison, the Fe- and Cu-based catalysts (i.e. Fe/ZIF-1000 and Cu/ZIF-1000) are prepared using a method similar to Co/ZIF-1000. As shown in their TEM and Aberration-corrected HAADF-STEM images (Figure S10 for Fe/ZIF-1000 and Figure S11 for Cu/ZIF-1000), as well as the XRD patterns, XPS spectra and EXAFS spectra (Figure S12 for Fe/ZIF-1000 and Figure S13 for Cu/ZIF-1000), they are Fe- and Cu-based single atom catalysts.

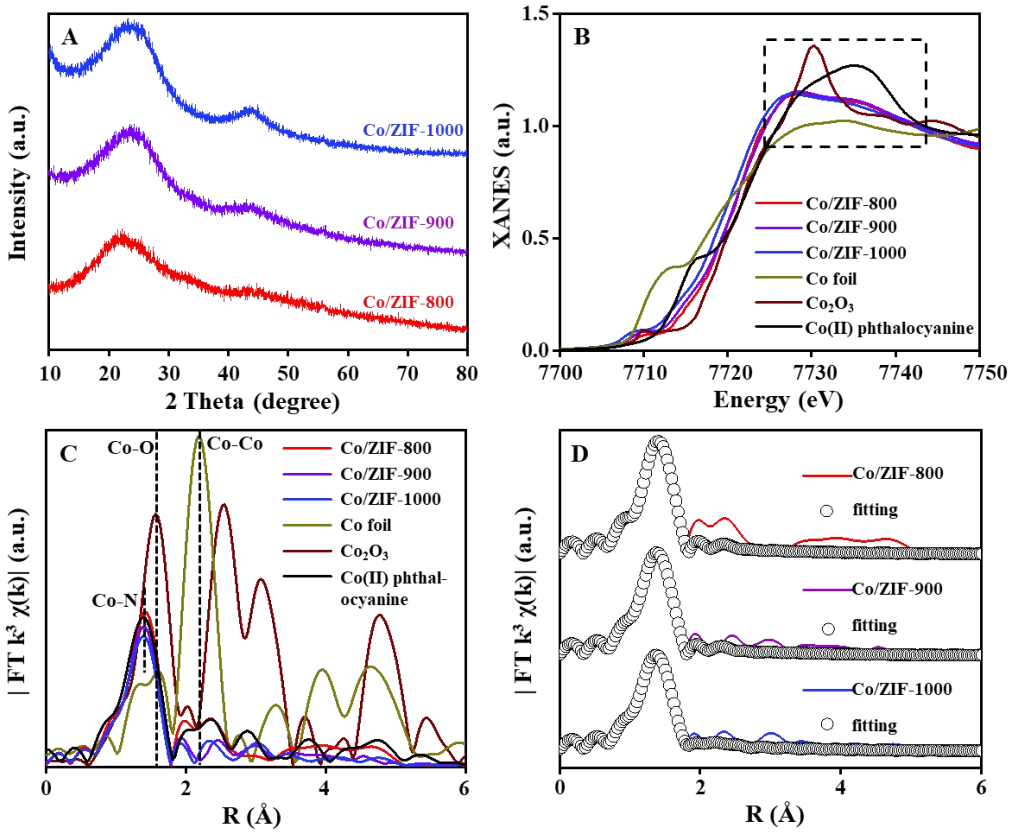

Figure 3. Chemical state and coordination information of Co SACs. (A) XRD patterns, (B) Co K edge X-ray absorption near-edge spectroscopy spectra, (C) K^3-weighted χ(k) function of EXAFS spectra, and (D) EXAFS fitting curves of Co/ZIF-800, Co/ZIF-900 and Co/ZIF-1000.

The performances of various catalysts are evaluated in the oxidation of styrene. In the typical run, 50 mg catalyst are directly added to the mixture of 2.56 mmol styrene, 65 mmol acetonitrile and 7.68 mmol TBHP, and the moment when the temperature reaches 100 °C is regarded as the initial reaction time. Figure 4A and Figure 4B show the styrene conversion and SO selectivity with reaction time over various catalysts, respectively. As expected, Co/ZIF-1000 simultaneously exhibits excellent activity and

SO selectivity. After a reaction time of 8 hours, the styrene conversion and the SO selectivity achieves 99.9 % and 71 % on Co/ZIF-1000, respectively. In comparison, Co/ZIF-800 and Co/ZIF-900 display comparable SO selectivity but obviously lower styrene conversion with Co/ZIF-1000, which can be explained by the relative higher energy barrier for SO formation over Co-N_4 sites than over Co-N_3 sites. Moreover, although Fe/ZIF-1000 and Cu/ZIF-1000 also possess high activity in this reaction, they exhibit undesirable SO selectivity. In a further analysis of the by-products (Figure 4C and Figure 4D), the low SO selectivity over Fe/ZIF-1000 and Cu/ZIF-1000 is mainly attributed to the massive formation of BA and its overoxidation derivative benzoic acid (BAD), which is in line with the calculation results. For comprehensive comparison, TOF values are calculated with the data extracted at a reaction time of 2h (Table S2). Co/ZIF-1000 exhibits a TOF of 19.3 $mol_{SO} \cdot mol_{Co}^{-1} \cdot h^{-1}$, which is 1.5 times, 2.3 times, 1.1 times and 14.8 times as that of Co/ZIF-900, Co/ZIF-800, Cu/ZIF-1000 and Fe/ZIF-1000, respectively. After a reaction time of 8 hours, a high SO yield of 71 % is reached over Co/ZIF-1000, which is 1.45 times, 1.9 times, 3.9 times and 36 times as that of Co/ZIF-900, Co/ZIF-800, Cu/ZIF-1000 and Fe/ZIF-1000, respectively (Figure 4E). Figure 4F shows the reusability of Co/ZIF-1000, where the Co/ZIF-1000 is filtered, dried and used without further treatment. The conversion of styrene and SO selectivity over Co/ZIF-1000 are decreased slightly after five consecutive runs, suggesting the high durability of Co/ZIF-1000 in this application. Figure S14 shows the XRD pattern, TEM image,

STEM image and EXAFS spectrum of Co/ZIF-1000 after reusability test. It can be observed that Co atoms still exist as isolated Co sites in the spent Co/ZIF-1000, which explains the high stability of Co/ZIF-1000 in the reusability test.

Table S2 compares the performance of Co/ZIF-1000 with recently reported high-performance catalysts for styrene epoxidation. As a result, the performance of Co/ZIF-1000 (SO yield, 71 %; TOF, 19.3 $mol_{SO} \cdot mol_{Co}^{-1} \cdot h^{-1}$) is one of the best results among these studies. It should be noticed that the severe decline of SO selectivity is frequently observed with respect to the reaction time, since the overoxidation of SO, especially for Fe- and Cu- based catalysts. [2,9,16,26] This phenomenon can be also observed in the reported high-performance Fe SACs [2] and our Cu/ZIF-1000. Over Co/ZIF-1000, this is significantly improved, as shown in Figure 4B. We suppose this may benefit from the relative low energy of SO with Co sites, which allows rapid SO desorption from active sites. Table 2 further exhibits the performance of other Co-based catalysts in similar operation condition (50 mg catalysts, reaction at 100 °C for 8 hours), including cobalt (II) phthalocyanine, cobalt nitrate, Co_2O_3 and Co_3O_4. It can be discovered that Co/ZIF-1000 exhibits much better performance, even the metal loading is very limited. In recent years, SACs have attracted greatly attentions in various applications, due to their high atom utilization, remarkable novel catalytic activity, and conformational flexibility. [27-29] However, the rational design of SAC remains an open challenge. [27] This present contribution provides an example to explore desirable SAC for specific reactions.

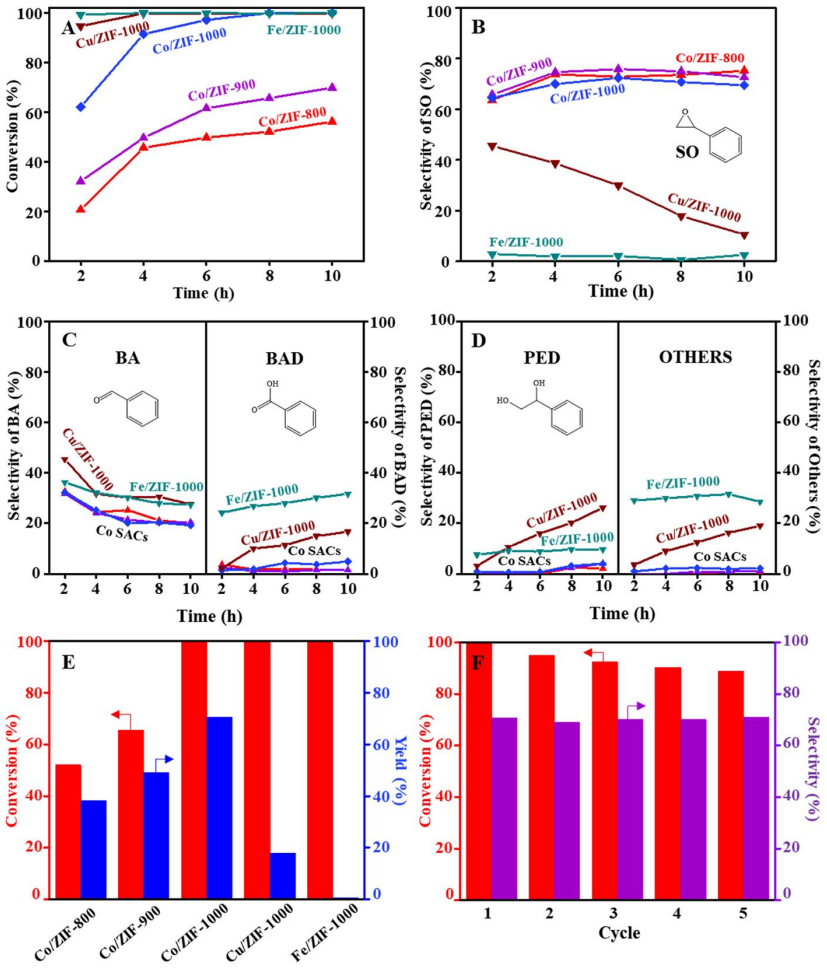

Figure 4. Catalytic evaluation. Reaction condition: 2.56 mmol styrene, 50 mg catalysts, 65 mmol acetonitrile, 7.68 mmol TBHP, 100 °C. (A) conversion of styrene and (B) selectivity of SO with reaction time over various catalysts. Selectivity of (C) direct oxidation products (BA and BAD), (D) overoxidation derivative of SO (PED) and other products with reaction time over various catalysts. (E) The comparison of SO yield for various samples, with a reaction time of 8 hours. (F) reusability test of five consecutive runs.

Table 2. Catalytic activity of other samples for epoxidation of styrene with TBHP.

Catalyst	Conv. (%)[a]	Sel. SO (%)[a]	Yield (SO, %)[a]	TOF ($mol_{SO} \cdot mol_{Co}^{-1} \cdot h^{-1}$)[b]
Co/ZIF-1000	99.9	71	71	19.3
Co/ZIF-900	65.5	75	49	12.5
Co/ZIF-800	52.0	74	38	8.3
Cu/ZIF-1000	99.9	18	18	17.5
Fe/ZIF-1000	99.9	2	2	1.3
Cobalt (II) phthalocyanine	99.9	trace	-	-
$Co(NO_3)_2$	99.9	trace	-	-
Co_2O_3	96.4	31	30	-
Co_3O_4	61.3	63	39	-

[a] reaction condition: 2.56 mmol styrene, 50 mg catalysts, 65 mmol acetonitrile, 7.68 mmol TBHP, 100 ℃, 8h. [b] TOF values are calculated with the data extracted at a reaction time of 2h.

3. Conclusion

To achieve efficient preparation of styrene oxide via epoxidation of styrene with TBHP, Co single-atom catalyst with vacancy-defect (Co/ZIF-1000) has been prepared in accordance with the prediction of DFT calculation. After a reaction time of 8 hours at 100 ℃ over Co/ZIF-1000, styrene is nearly totally converted and the SO selectivity achieves 71 %, which is one of the best results, to our knowledge, thereby suggesting its potential application in SO fabrication.

4. Experimental Section

Preparation of catalysts: The employed transition metal single atom catalysts were prepared using the host-guest method. [22, 23] Here, 100 mg ZIF-8 was added to a mixture of 10 ml n-hexane solution and 60 μL of cobaltous nitrate aqueous solution (0.1 $g \cdot ml^{-1}$). This mixture was then stirred for six hours at room temperature, centrifuged and dried in vacuum at 80 °C for 12 hours. The obtained powders were pyrolyzed at 800, 900 and 1000 ℃ for one hour under Ar atmosphere, and labelled Co/ZIF-800, Co/ZIF-900 and Co/ZIF-1000, respectively. The reference catalysts Fe/ZIF-1000 and Cu/ZIF-1000 were prepared using a process similar to that used for Co/ZIF-1000, using ferric nitrate and cupric nitrate as precursors, respectively. Other reference catalysts are purchased from commercial companies and used without further treatment.

Epoxidation of styrene: Typically, the reaction was conducted in a 20 ml Teflon-lined stainless-steel autoclave. 50 mg of the catalyst was added to a mixture of 2.56 mmol styrene, 65 mmol acetonitrile and 7.68 mmol TBHP. Then, the reaction was carried out at 100 °C in an electric oven. After the reaction, the mixture was analysed by Agilent 5977B GC/MS and Agilent 8890 GC systems. Dodecane was used as an internal standard.

Details of the DFT calculations, synthesis process, characterizations and catalytic evaluations are presented in the Supporting Information.

ASSOCIATED CONTENT

Supporting Information

Additional experimental details, materials, and method; Supplementary figures for additional experimental results including the models used for DFT calculations, detailed characterization of the catalysts (TEM images, XRD pattern, XPS spectra, Raman spectra, N_2 isotherm, etc.); Parameter table for structural fitting, and comparison table of Co/ZIF-1000 with other reported catalysts for epoxidation of styrene. (PDF)

AUTHOR INFORMATION

Corresponding Authors

Yi Wang — State Key Laboratory of Photoelectric Technology and Functional Materials, International Collaborative Center on Photoelectric Technology and Nano Functional Materials, Institute of Photonics and Photon-Technology, Northwest University, Xi'an, Shaanxi 710069, China. E-mail: yi.wang@nwu.edu.cn

Kunyue Leng — State Key Laboratory of Photoelectric Technology and Functional Materials, International Collaborative Center on Photoelectric Technology and Nano Functional Materials, Institute of Photonics and Photon-Technology, Northwest University, Xi'an, Shaanxi 710069, China. E-mail: lengky@nwu.edu.cn

Jinbo Bai — Laboratory MSSMat, CNRS UMR 8579, Ecole CentraleSupélec, Université Paris-Saclay, 8-10 rue Joliot-Curie, Gif-sur-Yvette 91190, France. E-mail: jinbo.bai@centralesupelec.fr

Author Contributions

All authors have given approval to the final version of the manuscript. ‡These authors contributed equally.

ACKNOWLEDGMENT

This work is financial supported by the National Natural Science Foundation of China (51873174), and the Scientific Research Project of Education Department of Shaanxi Province (20JK0945). The authors thank the photoemission endstations beamline 1W1B station in the Beijing Synchrotron Radiation Facility (BSRF), BL14W1 at the Shanghai Synchrotron Radiation Facility, and BL10B and BL11U at the National Synchrotron Radiation Laboratory for help with the characterizations.

ABBREVIATIONS

BA, benzaldehyde; SO, styrene oxide; BAD, benzoic acid; PED, 1-phenyl-2-ethanediol; TBHP, tert-butyl hydroperoxide; SAC, single atom catalyst.

REFERENCES

(1) Tian, S.; Wang, B.; Gong, W.; He, Z.; Xu, Q.; Chen, W.; Zhang, Q.; Zhu, Y.; Yang, J.; Fu, Q.; Chen, C.; Bu, Y.; Gu, L.; Sun, X.; Zhao, H.; Wang, D.; Li, Y. Dual-atom Pt heterogeneous catalyst with excellent catalytic performances for the selective hydrogenation and epoxidation. Nat. Commun. 2021, 12, 3181.

(2) Xiong, Y.; Sun, W.; Xin, P.; Chen, W.; Zheng, X.; Yan, W.; Zheng, L.; Dong, J.; Zhang, J.; Wang, D.; Li, Y. Gram-Scale Synthesis of High-Loading Single-Atomic-Site Fe Catalysts for Effective Epoxidation of Styrene. Adv. Mater. 2020, 32, 2000896.

(3) Banerjee, D.; Jagadeesh, R. V.; Junge, K.; Pohl, M.-M.; Radnik, J.; Brückner, A.; Beller, M. Convenient and mild epoxidation of alkenes using heterogeneous cobalt oxide catalysts. Angew. Chem. Int. Ed. 2014, 53, 4359-4363.

(4) Tian, S.; Peng, C.; Dong, J.; Xu, Q.; Chen, Z.; Zhai, D.; Wang, Y.; Gu, L.; Hu, P.; Duan, H.; Wang, D.; Li, Y. High-Loading Single-Atomic-Site Silver Catalysts with an Ag1–C2N1 Structure Showing Superior Performance for Epoxidation of Styrene. ACS Catal. 2021, 11, 4946-4954.

(5) Wang, Q.; Deng, X.; Chen, W.; Chen, P.; Liu, F.; Yin, S.-F. Bismuth complexes with N/S coordination based metallopolymer as highly efficient photocatalyst for selective oxidation of styrene. Fuel 2021, 302, 121127.

(6) Fu, H.; Huang, K.; Yang, G.; Cao, Y.; Wang, H.; Peng, F.; Wang, Q.; Yu, H. Synergistic Effect of Nitrogen Dopants on Carbon Nanotubes on the Catalytic Selective Epoxidation of Styrene. ACS Catal. 2020, 10, 129-137.

(7) Turner, M.; Golovko, V. B.; Vaughan, O. P. H.; Abdulkin, P.; Berenguer-Murcia, A.; Tikhov, M. S.; Johnson, B. F. G.; Lambert, R. M. Selective oxidation with dioxygen by gold nanoparticle catalysts derived from 55-atom clusters. Nature 2008, 454, 981-984.

(8) Cui, H.; Zhang, Y.; Qiu, Z.; Zhao, L.; Zhu, Y. Synthesis and characterization of cobalt-substituted SBA-15 and its high activity in epoxidation of styrene with molecular oxygen. Appl. Catal. B: Environ. 2010, 101, 45-53.

(9) Liu, J.; Meng, R.; Li, J.; Jian, P.; Wang, L.; Jian, R. Achieving high-performance for catalytic epoxidation of styrene with uniform magnetically separable CoFe2O4 nanoparticles. Appl. Catal. B: Environ. 2019, 254, 214-222.

(10) Shi, Z.-Q.; Dong, Z.-P.; Sun, J.; Zhang, F.-W.; Yang, H.-L.; Zhou, J.-H.; Zhu, X.-H.; Li, R. Filled cobalt nanoparticles into carbon nanotubes as a rapid and high-efficiency catalyst for selective epoxidation of styrene with molecular oxygen. Chem. Eng. J. 2014, 237, 81-87.

(11) Hu, R.; Yang, P.; Pan, Y.; Li, Y.; He, Y.; Feng, J.; Li, D. Synthesis of a highly dispersed CuO catalyst on CoAl-HT for the epoxidation of styrene. Dalton Trans. 2017, 46, 13463-13471.

(12) de Brito S. Neto, A.; Pinheiro, L. G.; Filho, J. M.; Oliveira, A. C. Studies on styrene selective oxidation over iron-based catalysts: Reaction parameters effects. Fuel 2015, 150, 305-317.

(13) Huang, C.; Zhang, H.; Sun, Z.; Zhao, Y.; Chen, S.; Tao, R.; Liu, Z. Porous Fe3O4 nanoparticles: Synthesis and application in catalyzing epoxidation of styrene. J. Colloid Interface Sci. 2011, 364, 298-303.

(14) Liu, J.; Chen, T.; Jian, P.; Wang, L.; Yan, X. Hollow urchin-like NiO/NiCo2O4 heterostructures as highly efficient catalysts for selective oxidation of styrene. J. Colloid Interface Sci. 2018, 526, 295-301.

(15) Liu, J.; Wang, H.; Ye, R.; Jian, P.; Wang, L. Promotional effect of Mn-doping on the catalytic performance of NiO sheets for the selective oxidation of styrene. J. Colloid Interface Sci. 2021, 585, 61-71.

(16) Gu, B.; bai, J.; Yang, w.; Li, C. Synthesis of ANA-zeolite-based Cu nanoparticles composite catalyst and its regularity in styrene oxidation. Microporous Mesoporous Mater. 2019, 274, 318-326.

(17) Tian, S.; Fu, Q.; Chen, W.; Feng, Q.; Chen, Z.; Zhang, J.; Cheong, W.-C.; Yu, R.; Gu, L.; Dong, J.; Luo, J.; Chen, C.; Peng, Q.; Draxl, C.; Wang, D.; Li, Y. Carbon nitride supported Fe2 cluster catalysts with superior performance for alkene epoxidation. Nat. Commun. 2018, 9, 2353.

(18) Yang, R. A.; Sarazen, M. L. Reaction pathways and deactivation mechanisms of isostructural Cr and Fe MIL-101 during liquid-phase styrene oxidation by hydrogen peroxide. Catal. Sci. Technol. 2021, 11, 5282-5296.

(19) Zhang, Y.; Li, Y.-X.; Liu, L.; Han, Z.-B. Palladium nanoparticles supported on UiO-66-NH2 as heterogeneous catalyst for epoxidation of styrene. Inorg. Chem. Commun. 2019, 100, 51-55.

(20) Saikia, M.; Kaichev, V.; Saikia, L. Gold nanoparticles supported on nanoscale amine-functionalized MIL-101(Cr) as a highly active catalyst for epoxidation of styrene. RSC Adv. 2016, 6, 106856-106865.

(21) Żółtowska, S.; Miñambres, J. F.; Piasecki, A.; Mertens, F.; Jesionowski, T. Three-dimensional commercial-sponge-derived Co3O4@C catalysts for effective treatments of organic contaminants. J. Environ. Chem. Eng. 2021, 9, 105631.

(22) Qu, Y.; Li, Z.; Chen, W.; Lin, Y.; Yuan, T.; Yang, Z.; Zhao, C.; Wang, J.; Zhao, C.; Wang, X.; Zhou, F.; Zhuang, Z.; Wu, Y.; Li, Y. Direct transformation of bulk copper into copper single sites via emitting and trapping of atoms. Nat. Catal. 2018, 1, 781-786.

(23) Ma, S.; Han, Z.; Leng, K.; Liu, X.; Wang, Y.; Qu, Y.; Bai, J. Ionic Exchange of Metal-Organic Frameworks for Constructing Unsaturated Copper Single-Atom Catalysts for Boosting Oxygen Reduction Reaction. Small 2020, 16, 2001384.

(24) Hu, F. X.; Hu, T.; Chen, S.; Wang, D.; Rao, Q.; Liu, Y.; Dai, F.; Guo, C.; Yang, H. B.; Li, C. M. Single-Atom Cobalt-Based Electrochemical Biomimetic Uric Acid Sensor with Wide Linear Range and Ultralow Detection Limit. Nano-Micro Lett. 2021, 13, 7.

(25) Guo, Y.; Liu, F.; Feng, L.; Wang, X.; Zhang, X.; Liang, J. Single Co atoms anchored on nitrogen-doped hierarchically ordered porous carbon for selective hydrogenation of quinolines and efficient oxygen reduction. Chem. Eng. J. 2022, 429, 132150.

(26) Bepari, R. A.; Bharali, P.; Das, B. K. Controlled synthesis of α- and γ-Fe_2O_3 nanoparticles via thermolysis of PVA gels and studies on α-Fe_2O_3 catalyzed styrene epoxidation. *J. Saudi Chem. Soc.* **2017**, 21, 170-178.

(27) Hwa Jeong, G.; Chuan Tan, Y.; Tae Song, J.; Lee, G.-Y.; Jin Lee, H.; Lim, J.; Young Jeong, H.; Won, S.; Oh, J.; Ouk Kim, S. Synthetic Multiscale Design of Nanostructured Ni Single Atom Catalyst for Superior CO2 Electroreduction. Chem. Eng. J. 2021, 426, 131063.

(28) Kim, I.; Lim, J. Kim, S. Discovery of Single-Atom Catalyst: Customized Heteroelement Dopants on Graphene. Acc. Mater. Res. 2021, 2, 394-406.

(29) Lee, D. H.; Lee, W. J.; Lee, W. J.; Kim, S. O.; Kim, Y.-H. Theory, Synthesis, and Oxygen Reduction Catalysis of Fe-Porphyrin-Like Carbon Nanotube. Phys. Rev. Lett. 2011, 106, 175502.

For Table of Contents Only